

A THEORETICAL CALIBRATION OF THE PLANETARY NEBULAR
COSMIC DISTANCE SCALEMICHAEL A. DOPITA,¹ GEORGE H. JACOBY,² AND E. VASSILIADIS¹*Received 1991 July 8; accepted 1991 October 7*

ABSTRACT

We have computed an extensive grid of optically thick model planetary nebulae (PN) in order to determine the extent to which the emission-line fluxes used in the planetary nebular distance scale are affected by the stellar effective temperature and the nebular and stellar metallicity. We conclude that the nebular flux in the $H\beta$ line is closely related to the luminosity of the central star, but that the more commonly used flux in the $[O\ III]$ line at 5007 Å can also be calibrated to give a reliable estimate of this quantity. We also present a simple method for determining the stellar effective temperature and the luminosity, and the nebular metallicity using only the Balmer lines and the lines of $[O\ III]$ in the optical.

As an absolute calibration of the planetary nebular distance scale, we have derived the excitation, extinction, and metallicity-corrected cutoff in the luminosity function for the planetary nebulae in both the Small and Large Magellanic Clouds and have derived the true distance modulus to the LMC by a new hydrogen-reignition clump-fitting technique based on self-consistent helium-burning evolutionary models for the central stars. On this basis we estimate the distance to the LMC to be 47.2 ± 3.3 kpc. Using the cutoffs in the observed luminosity functions of the Galactic Bulge PN, M31, and the Virgo Cluster, and correcting the absolute luminosities of the planetary nebulae nuclei (PNn) for both stellar age and metallicity effects, we have been able to derive relative distance moduli of these systems. We find the following true distance moduli ($m - M$)₀: LMC 18.37 ± 0.15 , SMC 18.72 ± 0.15 , Galactic Center 14.4 ± 0.2 , M31 24.14 ± 0.20 and Virgo Cluster 30.86 ± 0.25 . In all cases where Cepheid distances are known, we find a $+0.14$ mag zero-point offset with respect of the PN cosmic distance scale. Correcting to the Cepheid scale, we infer that Virgo lies at a distance of 15.8 ± 1.8 Mpc, which would imply a global Hubble constant of 84 ± 11 km s⁻¹ Mpc⁻¹.

We conclude that the principle uncertainty in the PN cosmic distance scale is in our knowledge of the intrinsic upper luminosity cutoff of the PN central stars, which is critically dependent upon the stellar age, and the treatment of mass loss in the stellar evolutionary models.

Subject headings: distance scale — galaxies: distances and redshifts — Magellanic clouds — planetary nebulae: general — stars: fundamental parameters

1. INTRODUCTION

The luminosity function of PN has been shown to be a very promising extragalactic distance indicator (Jacoby, Ciardullo, & Ford 1990). Up to the present time, no compelling evidence for a metallicity dependence on the luminosity function of PN has yet been detected (Jacoby, Ciardullo, & Ford 1988; Jacoby, Walker, & Ciardullo 1990). However, before this indicator achieves total acceptance, it must be shown that any sensitivity to metallicity of the host galaxy stellar population is either negligible or can be calibrated and removed. A comparable situation exists for other common and more widely known candles such as RR Lyrae stars and Cepheids.

Jacoby (1989) suggested that the peak $[O\ III]$ luminosities of an ensemble of PN experience a modest $\sim Z^{0.5}$ dependence. Provided that the method is applied differentially, between objects with metallicity differences of 30% or less, then errors from this source would be relatively unimportant. This is the case, for example, when distances for giant Virgo ellipticals in the Virgo Cluster are derived using the bulge of M31 as a calibrator. However, any attempt to apply the technique to a

wider range of metallicities could lead to a significant error if the method is this sensitive to metallicity variations.

Jacoby's (1989) conclusion was based on a very limited numerical experiment in which it was assumed that the luminosities of the central stars are unaffected by metallicity. Sandage & Tammann (1990), however, correctly point out that the dependence of the central star core mass and luminosity with metallicity cannot be ignored if the models of Lattanzio (1986) are adopted. Those models, which refer to giant stars, rather than to PNn suggest that the core masses of central stars should decrease with metallicity such that $L \sim Z^{-0.25}$. More recent models by Brocato et al. (1989) yield similar expectations but with a stronger $L \sim Z^{-0.5}$ dependence. Thus, to the extent that core mass on the giant branch and PNn core mass are related, the planetary nebula system (nebula plus exciting star) might be expected to display a net power-law luminosity dependence with an index of between 0.0 (for the Brocato et al. model) and +0.25 (for the Lattanzio model).

In this paper, we examine the effects on the luminosity of PN in more detail using improved nebular modeling techniques (see § 2). In particular, we consider the behavior of the $[O\ III]$ and $H\beta$ emission lines, which have both been used as distance estimators in the past (Pottasch 1990). In addition, we consider the effects of metallicity variations on the mass of the central star. Thus, the modeled planetary nebula is treated as a self-consistent system. The model results provide the added bonus that, provided that the nebular temperature is known, it is

¹ Mount Stromlo and Siding Springs Observatories, Institute of Advanced Studies, The Australian National University, Private Bag, Weston Creek P.O., ACT 2611, Australia.

² Kitt Peak National Observatory, National Optical Astronomy Observatories, Box 26732, Tucson, AZ 85726-6732.

possible to derive the nebular metallicity, and the temperature and luminosity (and therefore mass) of the central star from minimal spectroscopic data.

2. PHOTOIONIZATION MODELING

Recently, Dopita & Meatheringham (1991a, b), have derived the stellar and nebular parameters of a large sample of Magellanic Cloud PN through self-consistent photoionization modeling. This work demonstrated that, for the optically thick PN in the Magellanic Clouds, at least, the stellar parameters are simply related to the excitation class, E , defined as a continuous variable by Dopita & Meatheringham (1990):

$$E = 0.45\{F(5007)/F(H\beta)\}, \quad 0.0 < E < 5.0,$$

$$E = 5.54\{0.78 + F(4686)/F(H\beta)\}, \quad 5.0 \leq E < 10.0, \quad (2.1)$$

with this definition, a least-squares fit to some 66 objects gives

$$\log(T_{\text{eff}}) = (4.489 \pm 0.017) + (0.1124 \pm 0.0025)E$$

$$- (0.00172 \pm 0.00037)E^2, \quad (2.2)$$

with a correlation coefficient of 0.98, and, with a correlation coefficient of 0.96:

$$\log(L/L_{\odot}) = \log(L_{H\beta}/L_{\odot}) + (2.32 \pm 0.02)$$

$$- (0.179 \pm 0.016)E + (0.035 \pm 0.004)E^2$$

$$- (0.00166 \pm 0.00035)E^3 \quad (2.3)$$

For Magellanic Cloud abundances, these equations provide a useful transformation between the parameters of the "observed" Hertzsprung-Russell (H-R) plane; $\log(L_{H\beta}/L_{\odot})$ and E , and the "theoretical" H-R parameters; $\log(L/L_{\odot})$ and $\log(T_{\text{eff}})$. However, at other metallicities these simple relationships will break down, in particular, in the excitation class range $0.0 < E < 5.0$, because the $[O\text{ III}]/H\beta$ ratio is itself dependent on metallicity as well as upon the stellar temperature. It is therefore important to investigate the metallicity dependence before drawing general conclusions.

To this aim we have constructed a grid of model PN covering a range of stellar temperatures and metallicities using the generalized modeling code MAPPINGS (Binette, Dopita & Tuohy 1985). In general, the spectrum of an optically thick ionized region depends not only on these, but also upon the ionization parameter, Q , defined as (Evans & Dopita, 1985) as $Q = N_{\text{Ly-c}}/4\pi\langle r^2\rangle N_{\text{H}}$, where $N_{\text{Ly-c}}$ is the number of Lyman continuum photons emitted by the central source, and $\langle r \rangle$ is the mean radius of the ionized nebula with hydrogen particle density N_{H} . Only the upper end of the luminosity function of PN is observed in external galaxies. These objects will have luminosities generally larger than $1000L_{\odot}$. For this group of PN in the Magellanic Clouds, Dopita & Meatheringham (1991a, b) found Q to lie in the range $6 \times 10^7 < Q < 6 \times 10^8 \text{ cm s}^{-1}$, with an average of $\sim 2 \times 10^8 \text{ cm s}^{-1}$. At these high values of the ionization parameter, and with the high temperatures of the central star which characterize PN, the ionization parameter has only a second-order effect on the output spectrum.

For our grid, we adopt values of the ionization parameter, stellar luminosity, and nebular gas pressure typical of the brighter PN in the Magellanic Clouds, or of the brighter PN in the Galactic Bulge (Webster 1988; Pottasch & Acker 1989;

Tylenda et al. 1991), viz.:

$$L/L_{\odot} = 5000; \quad Q = 2 \times 10^8 \text{ cm s}^{-1}; \quad T_e N_{\text{H}} = 10^8 \text{ K cm}^{-3}.$$

With these parameters, we computed the emission line spectrum of isobaric model PN in photoionization equilibrium. The central star was assumed to have a blackbody distribution in frequency. Stars with effective temperature lower than 10^5 K have the spectrum cut off above 4 Ryd to simulate He^+ blanketing. To be sure, this may appear to be a rather crude approximation to the ionizing spectrum, but this has been found to work very satisfactorily in the case of the Magellanic Cloud PN, and there remain important uncertainties and disagreements within and between the various model atmosphere computations. In particular, the importance of non-LTE effects, and our knowledge of the effect of the extension of the atmosphere by stellar winds on the distribution of ionizing radiation has, in the past, been quite uncertain. Recent work on unified spherical non-LTE model atmospheres, which include a self-consistent treatment of both the photospheric and the wind regions show that the effect of this redistribution is to restore the emergent spectrum toward the blackbody distribution (Gabler, Kudritski, & Mendez 1991).

The "solar" abundance set adopted has the following relative numbers of atoms, H:He:C:N:O:Ne:Mg:Si:S:Cl:Ar = 1:0.1:1.04 $\times 10^{-3}$:8.7 $\times 10^{-5}$:6.9 $\times 10^{-4}$:9.8 $\times 10^{-5}$:4.0 $\times 10^{-5}$:3.8 $\times 10^{-5}$:1.9 $\times 10^{-5}$:1.8 $\times 10^{-7}$:4.0 $\times 10^{-6}$. This is solar except for the C/O ratio, which is taken as 1.5 to approximately account for the dredge-up of carbon on the AGB. At high metallicity (defined by $[\text{Fe}/\text{H}]$ ratio, it is known that there are few, if any, C stars. This suggests that the C/O ratio is probably less than unity in these systems, which will have some effect on the $[O\text{ III}]$ flux computed from our models. Dopita & Meatheringham (1990, 1991a, b) have investigated this effect in the context of attempts to model type I PN in the Magellanic Clouds, and find that the temperature and optical spectrum is remarkably insensitive to the assumed C/O ratio. We return to this point in § 6.3, below, where we find the same result. In our grid of models the helium abundance is kept fixed with respect to hydrogen, and the abundances of the other elements are scaled with respect to this set. Families of models have been computed at 0.1, 0.15, 0.2, 0.3, 0.5, 0.7, 1.0, 1.5, and 2.0 times solar abundances. For each of these abundance sets, we have computed models with the following set of temperatures; 35,000, 40,000, 45,000, 50,000, 55,000, 60,000, 70,000, 80,000, 90,000, 100,000, 110,000, 120,000, and 140,000 K. For fixed central star luminosity, and over the whole abundance range, this temperature range encompasses the luminosity maximum in both the $H\beta$ and in the $[O\text{ III}] \lambda 5007$ lines.

3. RESULTS

3.1. The $H\beta$ Flux

Equation (2.3) implies that, for optically thick PN, the absolute $H\beta$ flux should be a reliable indicator of stellar luminosity, provided that the excitation class is known. Even in the cases where the excitation class is not known, it is still possible to compute an approximate luminosity, since the conversion efficiency from stellar luminosity to luminosity in the $H\beta$ line only varies by a factor of at most 2. From our grid, we find that the variation of this conversion efficiency is even less. In Figure 1, we show the conversion efficiency factor as a function of stellar effective temperature and of metallicity. The peak efficiency occurs at a stellar effective temperature of near 70,000 K, and a

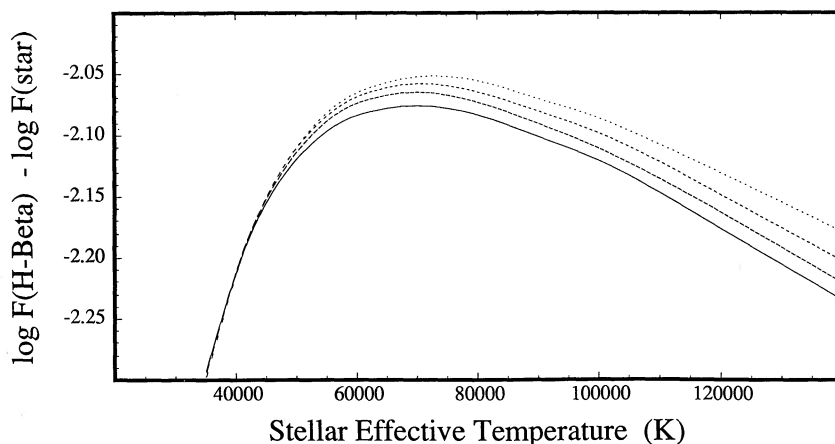


FIG. 1.—The conversion efficiency of stellar flux to $H\beta$ luminosity in optically thick PN models as a function of stellar effective temperature. The lines are for different O abundances in the nebula, as follows: *solid line*, 2 times solar; *long dashed line*, solar; *short dashed line*, 0.3 solar; and *dotted line*, 0.1 solar.

maximum of just under 1% of the luminosity of the star is converted to $H\beta$ photons. Note that the variation in the conversion efficiency factor is quite small. At a given temperature, metallicity variations of a factor of 10 make less than 10% change, and the variation with temperature is only 50%.

3.2. The [O III] Flux

The variation of the [O III] $\lambda 5007$ line intensity with metallicity and temperature is stronger and more complex than is the case for the Balmer lines. This is because the [O III] $\lambda 5007$ line is one of the most important coolants in the nebula. Figure 2 shows the luminosity conversion efficiency factor as a function of stellar effective temperature and of metallicity. At high metallicities, up to 15% of the luminosity of the central star is reradiated in the [O III] $\lambda 5007$ line alone! The effective temperature of the central star at which the luminosity conversion efficiency factor is maximized is somewhat dependent on the metallicity, ranging from 100,000 K at high metallicity, down to near 80,000 K for $\log [Z] = -1.0$. We therefore expect that the most [O III] luminous PN in any galaxy will be characterized by a fairly narrow range of effective stellar temperatures, corresponding to excitation classes 4–6, approximately, since objects with lower effective temperatures will have much lower

luminosity conversion efficiency factors and will therefore appear fainter. In the case of PN with much hotter central stars, the intrinsic luminosity of the central star will be lower as a result of hydrogen exhaustion.

The electron temperature as measured by the [O III] $\lambda\lambda 4363/5007$ ratio is sensitive to both metallicity and to stellar effective temperature. Hotter stars deliver a greater energy input to the nebula per phototization, resulting in hotter nebulae, and higher metallicity nebulae are cooled more efficiently by emission lines, producing cooler nebulae. On the other hand, Figures 1 and 2 show that the [O III]/ $H\beta$ ratio is a strong function of temperature and is also somewhat dependent on metallicity. This opens the possibility of using T_e and the [O III]/ $H\beta$ ratio as a diagnostic to localize PN on the $T_{\text{eff}}:\log [Z]$ plane. The results of our calculations are shown on Figure 3. Generally, the measured T_e and the [O III]/ $H\beta$ ratio can be used as diagnostic for both T_{eff} and $\log [Z]$. However, in the region $T_{\text{eff}} > 90,000$ K and $\log [Z] < -0.5$, the grid is not very useful for determination of the stellar temperature. However, this can be measured in this region using the He II $\lambda 4686/H\beta$ ratio, according to equations (2.1) and (2.2).

Figures 1–3 imply that in the case of optically thick PN, it is possible, using only spectrophotometric data between 4300

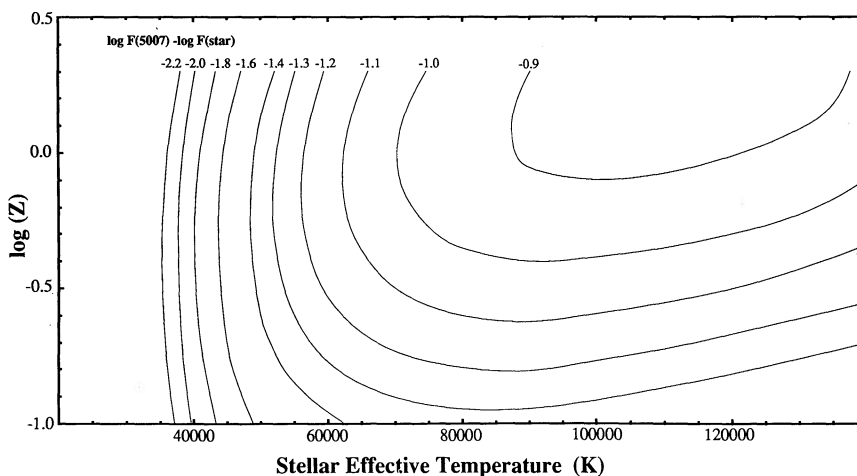


FIG. 2.—The conversion factor of stellar flux to [O III] $\lambda 5007$ line luminosity in optically thick PN models as a function of both stellar effective temperature and of metallicity.

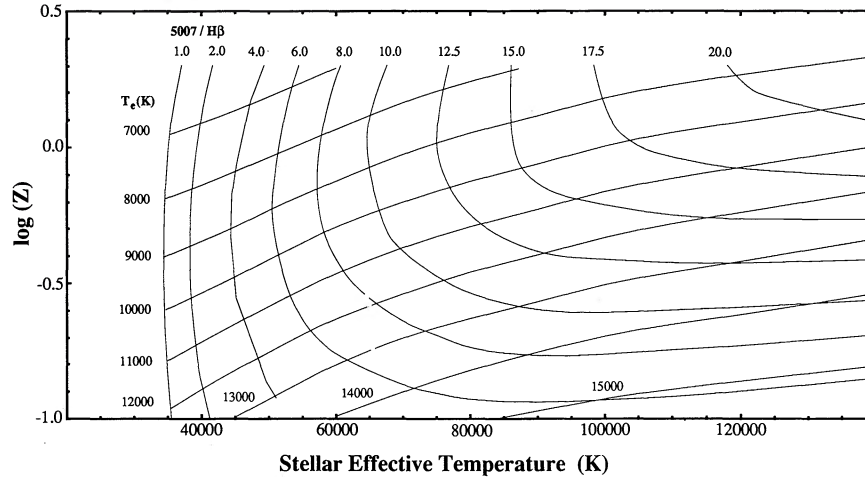


FIG. 3.—The grid defined by the electron temperature as measured by the $[\text{O III}]$ lines and by the $[\text{O III}]/\text{H}\beta$ line ratio as a function of both stellar effective temperature and of metallicity. Nebular and stellar conditions determined in this figure can be used to estimate the stellar luminosity using Fig. 2.

and 5100 \AA , to estimate the nebular metallicity and the position of the central star on the H-R diagram.

4. LUMINOSITY FUNCTIONS OF THE PN IN THE MAGELLANIC CLOUDS

The PN in the Magellanic Clouds, being bright, relatively nearby, and having low reddening, are an ideal group of objects against which to test theory. Jacoby, Walker & Ciardullo (1990) have already used these objects as a test of the PN distance scale and have given the $[\text{O III}]$ line fluxes for the PN listed in the luminosity-limited sample of Sanduleak, MacConnell, & Phillip (1978, hereafter SMP). For the majority of these objects, Meatheringham, Dopita, & Morgan (1988) and Wood et al. (1987) had already measured the $\text{H}\beta$ flux, and, for a large fraction of this sample, high-quality spectrophotometry exists (Monk, Barlow, & Clegg 1988; Meatheringham & Dopita 1991a, b; Dopita, Vassiliadis, & Morgan 1992).

Using these data, we have constructed (Figs. 4a–4b) the distribution of points on the emission-line flux: excitation class planes for both the $[\text{O III}]$ and $\text{H}\beta$ lines. As Dopita & Meatheringham (1990) have pointed out, these can be thought of as H-R diagrams transformed to observable coordinates. As expected, the $[\text{O III}]$ flux peak occurs near excitation class 6,

and the effect of the transformation of the H-R diagram implied in Figure 2 is quite evident.

The raw cumulative luminosity functions derived from the $[\text{O III}]$ and $\text{H}\beta$ line fluxes are shown in Figure 5a–5d. These have been derived from the observational data base of Meatheringham, Dopita, & Morgan (1988), Wood et al. (1987), Jacoby, Walker, & Ciardullo (1990) and Dopita et al. 1992. Extra $[\text{O III}]$ or $\text{H}\beta$ fluxes have been derived from the spectrophotometry of Monk, Barlow, & Clegg (1988) and Meatheringham & Dopita (1991a, b). In addition, for a small number of objects for which detailed spectrophotometry was unavailable, $\text{H}\beta$ fluxes have been estimated from the $[\text{O III}]$ fluxes of Jacoby, Walker, & Ciardullo (1990) using the excitation classes listed in Morgan (1984) and applying the transformations of equation (2.1).

In all cases, the upper part of the cumulative luminosity functions can be fitted by a straight line to give a well-defined upper luminosity cutoff, which is indicated in each case. This luminosity cutoff represents the observational basis of our distance estimates. However, in order to use it, corrections must be made for reddening, as well as for the efficiency of conversion of PNn luminosity to $[\text{O III}]$ or Balmer line photons.

As far as reddening is concerned, we have adopted a mean value of $c = 0.28$ for the LMC and $c = 0.26$ for the SMC

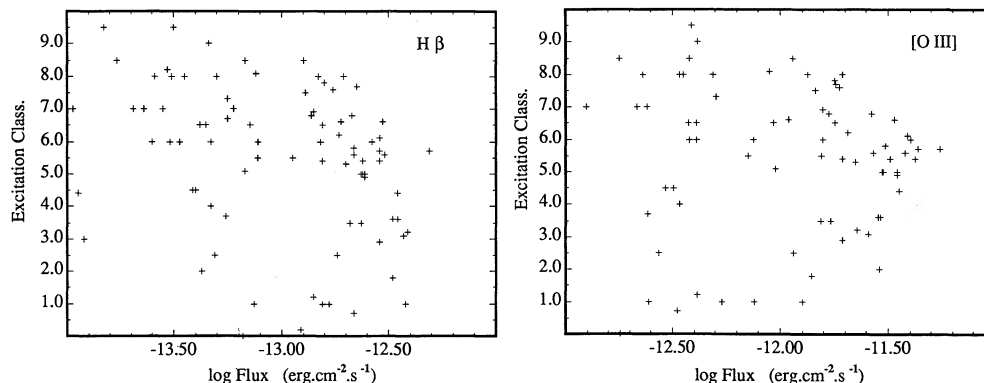


FIG. 4.—The raw $\text{H}\beta$ and $[\text{O III}]$ PN luminosities as a function of excitation class. Note that the $[\text{O III}]$ luminosities peak at excitation class 5–6.

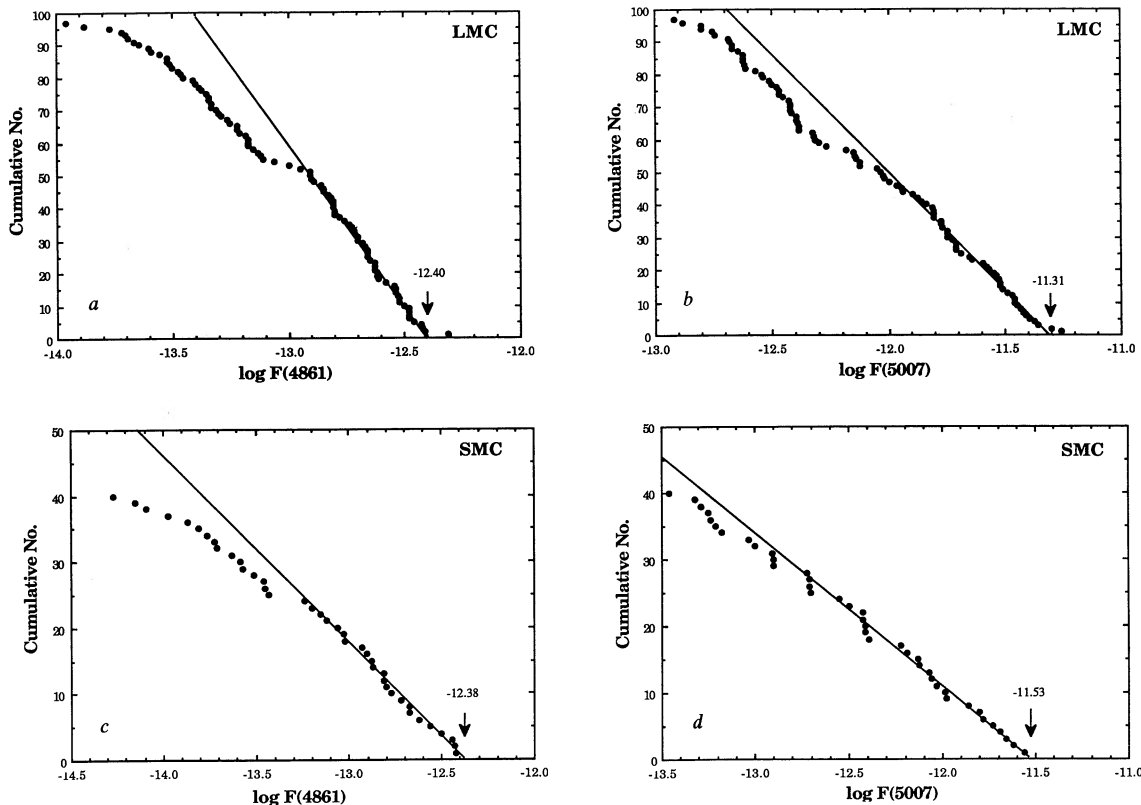


FIG. 5.—(a–d) The apparent H β and [O III] cumulative absolute luminosity functions for the LMC, and the SMC uncorrected for reddening. In each case the fit to the upper end of the function is shown, along with the inferred upper luminosity cutoff.

(Meatheringham & Dopita 1991a, b). These values correspond to $E(B-V) = 0.19$ and 0.17 mag, respectively, and are appreciably higher than the line-of-sight reddening of between 0.074 – 0.11 obtained for stars in the LMC (Caldwell & Coulson 1986; Conti, Garmany, & Massey 1986) or the SMC figure of 0.02 mag given by Gascoigne (1969). The implication is that the internal reddening by dust in the PN amounts to at least $E(B-V) = 0.10$ mag. Since the amount of internal dust is determined by dredge-up processes and ejection of carbon-rich matter into the nebular envelope, this term will show some dependence on metallicity and should also depend upon the mass of the central star. Fortunately, dust extinction is already sufficiently small that the differential in the internal reddening would not have a serious effect on distance estimates. However, a correction must be made for internal dust extinction in the derivation distances to other galactic systems.

In order to make a correction for the efficiency of conversion of stellar flux to observable photons, we adopt the mean O/H abundances of the PN in the Magellanic Clouds derived Meatheringham & Dopita (1991a, b), namely, 2.0×10^{-4} by number for the LMC, and 1.2×10^{-4} by number for the SMC. These correspond to $\log [\text{O}/\text{H}] = -0.54$ for the LMC, and -0.75 for the SMC. We should point out that these figures should be distinguished from the mean stellar metallicity, which is dominated by [Fe/H]. For these, we adopt values of $\log [Z] = -0.32$ (LMC) and -0.64 (SMC) (Russell & Dopita 1992).

From Figure 1, at these metallicities, the peak logarithmic conversion efficiency of stellar flux to flux in the H β line is -2.065 (LMC), and -2.05 (SMC). The peak conversion effi-

ciency of stellar flux to 5007 Å photons is conveniently given by

$$\{\log F(5007) - \log F(\text{star})\}_{\text{peak}} = -0.8791 + 0.1459 \log [\text{O}/\text{H}] - 0.3013 (\log [\text{O}/\text{H}])^2. \quad (4.1)$$

This functional form is derived from the table of models used to compute Figure 2 and implies a peak conversion rate of -1.046 (LMC) and -1.158 (SMC).

These figures can then be used to compute reddening corrected apparent upper PNn stellar luminosity cutoffs for the clouds, $\log (F^*)$, viz. -10.05 ergs $\text{cm}^{-2} \text{s}^{-1}$ (derived from H β for LMC), -9.99 ergs $\text{cm}^{-2} \text{s}^{-1}$ ([O III], LMC), -10.07 ergs $\text{cm}^{-2} \text{s}^{-1}$ (H β , SMC) and -10.12 ergs $\text{cm}^{-2} \text{s}^{-1}$ ([O III], SMC).

The method used to derive these cutoffs is identical to that which would be used in distant galaxies, where information about individual PN is lacking. However, in the case of the Magellanic Clouds, in most cases we know the reddening and stellar effective temperature applicable to each object. The observed luminosity functions can therefore be corrected on a point-by-point basis using Figures 1–3. When this is done, we derive the correlation between inferred stellar luminosities shown in Figure 6. As can be seen, the correlation is very good, except for a few discrepant points above and to the left of the line, which correspond to PN which are optically thin. We may therefore conclude that the metallicity and temperature corrections to the apparent luminosities appear to be correct for both the [O III] and H β lines.

In Figure 7, we show the reddening corrected cumulative

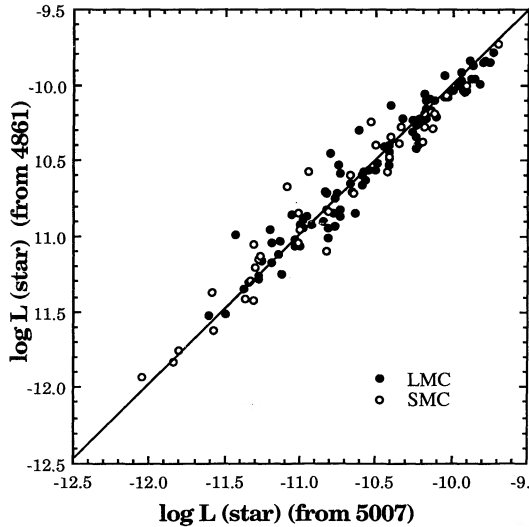


FIG. 6.—The relationship between apparent reddening-corrected stellar fluxes of individual PN in the LMC and the SMC derived from the [O III] line fluxes, or from the $H\beta$ line fluxes, using the relationships of Figs. 1–3. The units of flux are $\text{ergs cm}^{-2} \text{s}^{-1}$. The points which lie some distance above and to the left of the relationship are in all cases optically thin PN. It is clear that either line can be used equally well to derive the stellar flux, indicating that the corrections for metallicity and excitation are good.

stellar luminosity functions derived from the raw $H\beta$ and [O III] fluxes. The luminosity functions derived from the two lines are, to all intents and purposes, identical. The rollover in the slope of the luminosity function at lower luminosities is a consequence of incompleteness in the same. Note that, near the apparent upper stellar luminosity cutoff, $\log(F^*)$, the cumulative luminosity function is not so well fitted by a straight line. This is a consequence of the inclusion of low-temperature PNn with high internal reddening which, although not the most luminous objects in the raw sample, turn out to be the most luminous when corrected for extinction and the conversion efficiency to nebular emission. As a consequence, $\log(F^*)$ is somewhat higher than that inferred from the raw sample, $-9.80 \pm 0.03 \text{ ergs cm}^{-2} \text{ s}^{-1}$ (LMC) and $-9.90 \pm 0.06 \text{ ergs cm}^{-2} \text{ s}^{-1}$ (SMC). The difference between the apparent and

true $\log(F^*)$ is similar in both clouds, $+0.23$ for the LMC, and $+0.2$ for the SMC. If not accounted for, this could be an important source of zero-point error in more distant systems.

It remains to theoretically calibrate this cutoff in terms of absolute luminosity of the central star order to derive a PN distance to the Magellanic Clouds calibrated on purely theoretical grounds. In terms of absolute luminosity of the central star at the cutoff in the stellar luminosity function, L_{max} , and the observed luminosity cutoff, F^* , the distance scale is given by

$$D = 56.8(F^*/10^{-10} \text{ ergs cm}^{-2} \text{ s}^{-1})^{-1/2}(L_{\text{max}}/10^4 L_{\odot})^{1/2} \text{ kpc}.$$

5. EVOLUTIONARY MODELS OF THE PNn

The apparent intrinsic upper luminosity cutoff of the PNn is influenced by three major factors. First, the age of the stellar population, which determines the maximum mass of star that is currently proceeding through the PN phase. Second, the metallicity of this population, which influences both the core mass and the luminosity of the central star. Third, in cases where the stellar population is young, the rate of evolution across the H-R diagram. To a lesser extent the slope of the IMF will also help to determine the upper cutoff in young stellar populations (Shaw 1989).

The availability of evolutionary tracks for the PNn is somewhat limited (Paczynski 1971; Harm & Schwarzschild 1975; Schönberner 1981; Iben 1984; Wood & Faulkner 1986), and up to the present time fully self-consistent evolutionary tracks from the main sequence which cover a wide range of initial metallicity have been unavailable. As a consequence there remains considerable uncertainty in the relationship between the star on the zero-age main sequence and the PNn which it will produce in the fullness of time. In order to rectify this Vassiliadis & Wood (1992) have constructed fully self-consistent evolutionary models for stars from the zero-age main sequence all the way to the production of a white dwarf. These are fully described in that paper. Briefly, the important improvements that these models incorporate are as follows:

1. Abundances and opacities appropriate to SMC, LMC, and the Galaxy have been used (Huebner et al. 1977; Russell & Bessell 1989; Russell & Dopita 1990).

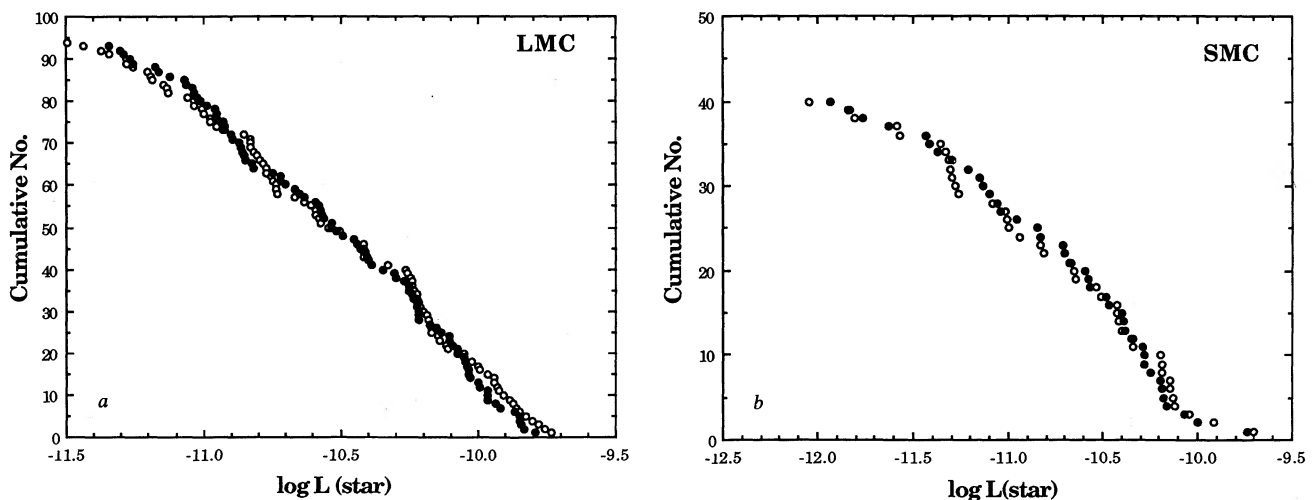


FIG. 7.—(a–b) The true cumulative apparent stellar luminosity functions for the LMC and SMC corrected for reddening, metallicity and excitation. The units of flux are $\text{ergs cm}^{-2} \text{ s}^{-1}$.

2. The updated Caughlan & Fowler (1988) reaction rates have been used.
3. The Castellani et al. (1985) treatment of semiconvection during the horizontal branch evolution has been incorporated.
4. Mass loss on the AGB and during the PN regime has been treated as well as is possible. In particular, the relation between mass loss and period of the thermally pulsing AGB star has been included according to the observational correlation (Wood 1991). Mass loss during the PN phase follows the semi-empirical relation derived from radiation-driven wind theory (Cerruti-Sola & Perinotto 1985; Pauldrach et al. 1989; Hutsemekers & Surdej 1989).

From the viewpoint of the present work, the most important factor in these calculations is the treatment of mass loss on the AGB. Note that no explicit dependence of this mass loss on metallicity has been included. Rather, this is included implicitly through the dependence of period on metallicity.

The results of these computations are summarized in Table 1, where the parameters are given at the time when the PNn reaches a temperature of 10,000 K during the transition to the left on the H-R diagram. The stellar age at this epoch is accurately expressed in terms of the initial mass, M , and the metallicity with respect to solar, $[Z]$, by

$$(\tau/\text{Gyr}) = 14.35[Z]^{0.195}(M/M_{\odot})^{-(3.4 + \log [Z])} \quad (5.1)$$

and the core mass M_c during the PN phase of evolution can be fitted by an expression of the form:

$$(M_c/M_{\odot}) = 0.493[Z]^{-0.035}[1 + 0.147(M/M_{\odot})] \quad (5.2)$$

The luminosity of the PNn depends upon whether these are on H-burning or He-burning tracks, which in turn depends on the phase of the thermal pulse at which the transition to PN occurs. Wood & Faulkner (1986) investigated this effect, but using a relatively crude treatment of mass loss, which critically affects the speed of evolution in the H-R diagram. For the hydrogen-burning objects, the evolution to high temperature occurs at an almost constant luminosity, L , which may be expressed in terms of the core mass by an expression similar to that given by Wood & Zarro (1981);

$$(L/L_{\odot}) = 57340[(M_c/M_{\odot}) - 0.507] . \quad (5.3)$$

TABLE 1
AGE, CORE MASS AND HYDROGEN-BURNING LUMINOSITIES
OF PLANETARY NEBULAE NUCLEI COMPUTED
BY VASSILIADIS AND WOOD (1992)

$\log [Z]$	ZAMS Stellar Mass (M_{\odot})	τ (Gyr)	$\log (L/L_{\odot})$ (H-burning)	$M_{\text{core}}(M_{\odot})$
Solar, 0.000	1.0	14.96	3.54	0.569
	1.5	3.65	3.73	0.600
	2.0	1.56	3.89	0.634
	2.5	0.956	3.98	0.677
LMC, -0.32	1.0	11.05	3.61	0.578
	1.5	3.11	3.88	0.620
	2.0	1.31	3.98	0.668
	2.5	0.784	4.01	0.679
SMC, -0.64	1.0	8.90	3.64	0.593
	1.5	2.64	3.86	0.640
	2.0	1.16	3.92	0.672
	2.5	0.661	4.15	0.692
Low, -1.21	1.0	7.21	3.78	0.623
	1.5	2.09	3.99	0.663

Note that the metallicity dependence of PNn luminosity is relatively weak. Equations (5.2) and (5.3) show that this dependence cannot be treated as a simple power law. However, if such a crude approximation must be made, then we have $L \sim Z^{-(0.3 \text{ to } 0.6)}$.

It is well known that the evolutionary track followed by the PNn on the H-R diagram is strongly dependent upon the phase of the thermal pulse cycle at which the PNn leaves the asymptotic giant branch (AGB) (e.g., Wood & Faulkner 1986). If the PNn leaves the AGB between thermal pulses, then it follows a classical hydrogen-burning path, which consists of a relatively constant-luminosity excursion to high temperatures, followed by a fading onto the contraction path to the white dwarfs (e.g., Paczyński 1971; Schönberner 1979, 1981, 1983). On the other hand, if the transition to a PN occurs during a thermal pulse, then the PNn leaves the AGB as a helium-burning object. In this case, the PNn fades as it makes its transition toward high temperatures. The luminosities of the helium-burning PNn are systematically lower than the hydrogen-burning case except near the point of departure from the AGB and following hydrogen reignition, where the luminosities approach that of equation (5.3). At a certain point, hydrogen is reignited, and the PNn luminosity increases again at almost constant effective temperature. The subsequent evolutionary track lies close to the corresponding hydrogen-burning track (Iben 1984; Wood & Faulkner 1986). Examples of helium-burning tracks are shown in Figure 8. In both the hydrogen- and helium-burning cases, the rate of evolution is very strongly dependent upon the core mass. However, this difference is most extreme for the hydrogen-burning objects. In the case of the helium-burning tracks, the reignition of hydrogen is associated with a marked slow-down in the rate of evolution. This turns out to be very important, as will be shown in the following section.

6. CALIBRATION OF THE PLANETARY NEBULA DISTANCE SCALE

One can, in principle, generate an [O III] luminosity function for planetary nebulae purely from theoretical considerations. Starting with some plausible initial mass function over the entire mass range applicable to PN progenitors (1–5 M_{\odot}), a scenario for the star formation history of the galaxy considered such as an exponentially decaying star formation rate or random bursts of star formation activity, a present-day stellar mass and age function can be derived. In turn, this can be combined with the evolutionary results given in equations (5.1)–(5.3) to yield a core-mass and age distribution for the central stars of PN for any metallicity. We then require to know whether the PNn are hydrogen or helium burning to predict the distribution of objects on the H-R diagram. Finally, the results of Figure 2 can be used to predict the corresponding luminosity distribution of objects in the [O III] line. A full analysis of this sort represents an effort beyond the scope of this work but will be attempted in a future paper.

It is more simple, however, to calculate the critical parameter in deriving extragalactic distances: the cutoff in the PNLF luminosity. In this section, we attempt to calibrate this for five specific groups of PN, those in the Large and Small Magellanic Clouds, the population of PN in the Galactic Bulge, the PN in M31, and finally the PN in the Virgo Elliptical Galaxies observed by Jacoby and his co-workers.

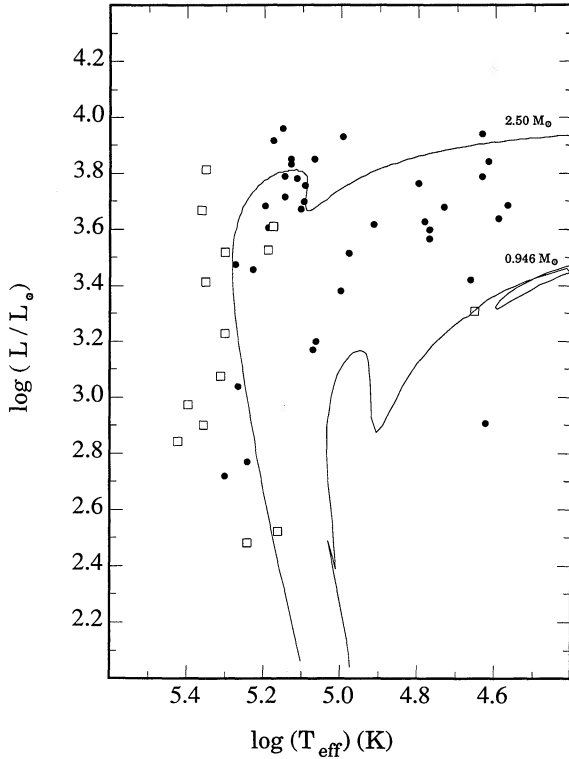


FIG. 8.—The theoretical and observed H-R diagram for the PNn in the Large Magellanic Cloud. The tracks are helium-burning models from Vassiliadis & Wood (1991) and refer to stars having initial masses of 0.945 and $2.5 M_{\odot}$, respectively. The observational points are for bright PNn in the LMC having optically thick nebulae and are taken from Dopita & Meatheringham (1991a, b). The type I objects are shown as open squares. The observed points have been scaled in luminosity in order to force a fit between the clump of objects at $4.0 \geq \log(L/L_{\odot}) \geq 3.7$; $5.2 \geq \log(T_{\text{eff}}) \geq 5.05$, and the position of the clump predicted in the region of hydrogen reignition on the helium-burning tracks.

6.1. PN in the Magellanic Clouds

Since the population of PN in the Magellanic Clouds is the most completely observed sample of objects at a fixed distance that we have available to us, clearly the calibration of the PN distance scale will depend critically upon this group. The observational H-R diagram for the LMC has been obtained by Dopita & Meatheringham (1991a, b) from nebular modeling. Since the points defined by optically thick nebulae are liable to be more accurate, we have selected only these for presentation in Figure 8. The sample consists of $\sim 50\%$ of the objects listed by Sanduleak, MacConnell, & Philip (1978). This sample should be complete in the area surveyed for optically thick nebulae having $\log(L/L_{\odot}) \geq 3.2$. Since the objects observed were drawn randomly from this sample, then the observed points should be representative of the sample as a whole above the same flux limit.

The distribution of the observed points cannot be explained if the PNn are hydrogen burning for a number of reasons.

First, since the mean age of the LMC stars is 3–8 Gyr (Stryker & Butcher 1981; Frogel & Blanco 1983; Hyland 1991), we might expect to see a large number of PN close to a luminosity of $\log(L/L_{\odot}) \sim 3.65$ – 3.75 , and a rapid drop in number density above this luminosity both because of the negative slope of the IMF, and because of the rapidly accelerating rate of evolution across the H-R diagram as one goes to

higher luminosity on the hydrogen-burning tracks. This is inconsistent with the observed cumulative luminosity distribution.

Second, the clump of points in the vicinity of $4.0 \geq \log(L/L_{\odot}) \geq 3.7$; $5.2 \geq \log(T_{\text{eff}}) \geq 5.05$ has no explanation on the basis of hydrogen-burning models which evolve through this portion of the H-R diagram in less than 1000 years.

Third, on the basis of hydrogen-burning models, the type I PN could not occur in the part of the H-R diagram that they are observed. These stars would have to have initial masses greater than $\sim 2.5 M_{\odot}$ to be able to evolve PNn with such high temperatures. These stars are not only rare compared with the lower mass PNn, but also they evolve exceedingly rapidly in the region $\log(T_{\text{eff}}) > 5.2$, and would fade to $\log(L/L_{\odot}) \leq 2$ within 1000 years. Even if we postulate a violent recent burst of star formation, we could not get the fraction of type I PN up to the $\sim 25\%$ which is observed.

All three of these problems has a natural solution if we postulate that the central stars are helium- rather than hydrogen-burners. First, the rate of evolution across the H-R diagram up to the point of hydrogen reignition is much less dependent on mass, decreasing only by a factor ~ 3 from a $1.0 M_{\odot}$ track to a $2.5 M_{\odot}$ track. Second, the rate of evolution slows down dramatically in the vicinity of the hydrogen reignition point. As an example, the $2.5 M_{\odot}$ LMC track shown on Figure 6 evolves from $\log(T_{\text{eff}}) = 4.5$ to the hydrogen reignition “dog-leg” in 2500 years. It then takes a further 5000 years negotiating the dog-leg before fading to $\log(L/L_{\odot}) = 2.6$ in another 5000 years. We therefore expect that the density of points observed near the reignition dog-leg will be of order 5 times higher than elsewhere. The same argument applies for the tracks of more massive stars giving rise to the type I PN. However, in these cases, the dog-leg occurs on the fading part of the evolutionary track and at lower luminosity.

The slower rate of evolution of the less massive stars is presumably the reason why the hydrogen reignition clump does not extend to lower luminosity for optically thick nebulae. The nebulae associated with these objects are less massive and would therefore be expected to have a larger velocity of expansion than higher luminosity PN having central stars with the same effective temperature. Given the slower rate of evolution across the H-R diagram, such nebulae will become optically thin, leading to a dramatic decline in their emission-line luminosities. Such nebulae would be relatively uncommon in the SMP sample, but should be plentiful in the Jacoby (1980) sample. Even within the SMP, evidence for such an effect is present when the kinematical data from Dopita et al. (1985) and Meatheringham et al. (1988) is compared with the effective temperatures of Dopita & Meatheringham (1991a, b). Both optically thin and optically thick objects show a linear correlation on the $v_{\text{exp}} : \log(T_{\text{eff}})$ plane, but each has a different slope. At an effective temperature of $\log(T_{\text{eff}}) = 4.4$, the mean expansion velocities of both classes of object are identical, $\sim 6 \text{ km s}^{-1}$. However, at a temperature of $\log(T_{\text{eff}}) = 5.0$, the optically thin objects have a mean expansion velocity of 37 km s^{-1} , while the optically thick objects have only reached a mean expansion velocity of 30 km s^{-1} .

The result that the PN stars appear to be helium- rather than hydrogen-burning is fundamental to our understanding of PN evolution in general. The thermal pulse which gives rise to helium-burning PN last ~ 10 times shorter than the interpulse duration. Clearly therefore, the enhanced luminosity during the thermal pulse is the most important factor leading

to the formation of the PN shell. The enhanced mass loss produced during the thermal pulse must occur at low velocity in order to be consistent with the observed expansion velocities of 6 km s^{-1} for the youngest PN.

The fact that the hydrogen reignition clump follows a well-defined trajectory in the H-R diagram allows us to calibrate the distance to the LMC by fitting the observed clump onto the trajectory estimated from the stellar models. This has been done in Figure 8 by increasing the luminosities estimated by Dopita & Meatheringham (1991a, b) by $+0.06$ dex. With this adjustment, the cumulative luminosity function for the optically thick PN is shown in Figure 9. Fitting a straight line to the upper section gives $\log(L_{\text{max}}/L_{\odot}) = 4.02 \pm 0.02$. Allowing for a ± 0.02 dex absolute calibration error in the luminosities used to derive this, and a further ± 0.02 dex error in conversion of the line flux to stellar flux, we estimate that the distance to the LMC is 47.2 ± 3.3 kpc. Expressed as a distance modulus, this corresponds to $(m - M)_0 = 18.37 \pm 0.15$. This is in good agreement with the revised Cepheid distance modulus of the LMC derived by Feast (1988), $(m - M)_0 = 18.52$.

The age of the stars which determine L_{max} can be estimated from equations (5.1)–(5.3) to be ~ 0.8 Gyr.

The distance of the SMC can be established in a differential manner with respect to the LMC. The observational value of $\Delta \log(F^*)$ between the LMC and the SMC is -0.07 ± 0.03 from the raw cumulative number/luminosity plot, or -0.10 ± 0.05 from the corrected version of the same plot. On the other hand, assuming the population which determines L_{max} has the same age in the SMC as in the LMC, then from equations (5.1)–(5.3) $\Delta \log(L_{\text{max}}/L_{\odot}) = 0.055 \pm 0.010$. From these numbers, the difference in the distance moduli of the two systems will be 0.35 ± 0.12 mag. Thus the distance modulus of the SMC is estimated to be 18.72 ± 0.17 corresponding to a distance of 55.5 ± 4.3 kpc. Again, the PN distance scale is somewhat “shorter” than the Cepheid scale, Feast (1988) finding $(m - M)_0 = 18.83 \pm 0.15$.

We summarize the adopted values of the key parameters

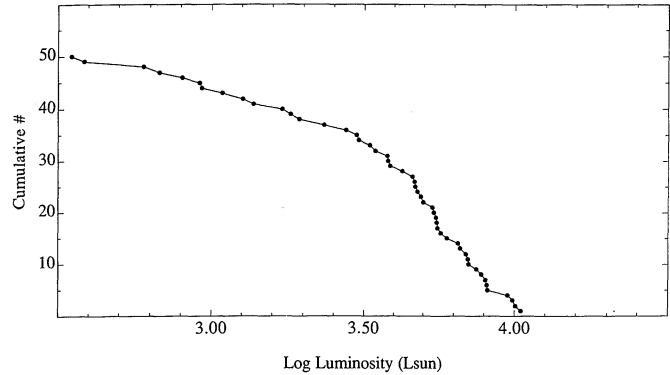


FIG. 9.—The intrinsic cumulative stellar luminosity function derived from the sample of optically thick nebulae in the LMC shown on Fig. 6. The well-defined upper luminosity cutoff is calibrated absolutely and is used as the basis of the distance estimates given in the remainder of this paper.

which determine the PN distance scale and the distance estimates themselves in Table 2.

6.2. The PN in the Galactic Bulge

The luminosity function of the PN in the Galactic Bulge can be investigated from their radio continuum emission, in particular, from their emission at 5 GHz (Gathier et al. 1983; Isaacman 1984; Zijlstra 1989; Pottasch 1990). The luminosity function derived by this route is essentially the same as the luminosity function derived from the $H\beta$ luminosity, since the radio continuum and the $H\beta$ emission are, to first-order, proportional to each other (Pottasch 1984, 1990);

$$S(5 \text{ GHz})/F(H\beta) = 2.82 \times 10^{12} [T_e/10^4 \text{ K}]^{0.53} Y \quad (6.1)$$

where $S(5 \text{ GHz})$ is the radio flux in mJy, $F(H\beta)$ is the $H\beta$ luminosity in $\text{ergs cm}^{-2} \text{ s}^{-1}$, T_e is the electron temperature, and Y is the number of electrons per hydrogen atom,

$$Y = 1 + N(\text{He}^+)/N(\text{H}) + 2N(\text{He}^{++})/N(\text{H}). \quad (6.2)$$

TABLE 2
THE PLANETARY NEBULA DISTANCE SCALE

Galaxy	log [Fe/H]	$E(B - V)$	log F^*		Age (Gyr)	log $L_{\text{max}} (L_{\odot})$	$(m - M)$	D (kpc)
			(app.)	(true)				
Galactic Bulge	+0.2	...	-8.50	-8.50	0.8	3.910	14.80	9.11
					5.0	3.737	14.36	7.46
LMC	-0.32	0.18	-10.03	-9.82	0.8	4.020	18.37 ± 0.15	47.2 ± 3.3
					Cepheid: ^{a,b,c}		18.51 ± 0.15	50.3 ± 3.4
SMC	-0.64	0.17	-10.10	-9.90	0.8	4.075	18.72 ± 0.17	55.5 ± 4.3
					Cepheid: ^{a,c}		18.83 ± 0.15	58.3 ± 3.9
M31	+0.3	0.11	-12.59	-12.59	5.0	3.614	24.28	718
					10.0	3.500	24.00	630
Virgo	+0.2 +0.3	0.02	-15.21	-15.21	5.0	3.737	31.14	16900
					10.0	3.500	30.55	12900
					Adopted:		30.86 ± 0.30	15000 ± 2000
					On Cepheid scale:		31.00 ± 0.30	15800 ± 2100

^a Feast 1988.

^b Laney & Stobie 1986.

^c Feast & Walker 1987.

^d Welch et al. 1986.

^e Freedman & Madore 1990.

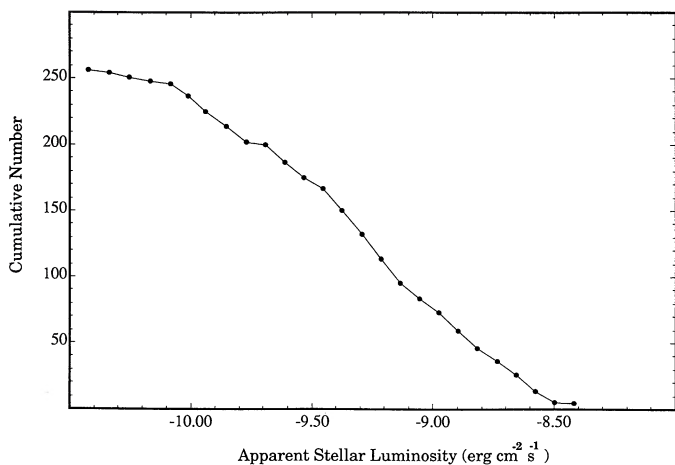


FIG. 10.—The cumulative apparent luminosity function for the PN in the Galactic Bulge

We have taken the 5 GHz luminosity distribution given in Pottasch (1990), adopted $\langle T_e \rangle \sim 9000$ K from Figure 3, used an average $\langle Y \rangle$ of 1.15 and have assumed at H β luminosity conversion factor of 2.11 from Figure 1 to derive a cumulative luminosity function for the Galactic Bulge. This is shown in Figure 10. Once again, the upper portion of the cumulative luminosity function for Galactic Center PN is a straight line with a well-defined upper luminosity cutoff at $\log F^* = -8.52 \pm 0.05$. The errors in this estimate do not account for selection effects in the sample, nor does it allow for the variation in the nebular temperature and the degree of helium ionization from object to object, each of which directly affects the radio flux. These effects are likely to somewhat increase our estimated errors.

The maximum luminosity, L_{\max} , is influenced by both the metallicity of the youngest stars in the Galactic Bulge, and also by their age. From the work of Webster (1988), we know that metal-rich PN are reasonably common in the Bulge, typically of order 1.5 times solar in terms of oxygen abundance. If recent star formation has occurred, and that L_{\max} is not determined by the mean age of the stellar population in the Bulge, and in this case we would only have to take into account the effect of metallicity on core mass in the determination of L_{\max} . However, this is not trivial. To do this, we have used equations (5.2) and (5.3) to derive the ratio of the L_{\max} for the Galactic Center and for the LMC. This procedure carries with it the caveat that equation (5.3) refers to hydrogen-burning stars, rather than helium-burning objects. However, the dogleg in the helium-burning tracks is caused by the reignition of hydrogen, which, if allowed to proceed to equilibrium, would return the PNn to the corresponding hydrogen burning track. Using a mean $\log(Z) = +0.20$ for the luminous Galactic Bulge PN, we find that the ratio of the L_{\max} for the Galactic Center to that of the LMC should be 0.78 ± 0.04 , giving a value of L_{\max} (Galactic Bulge) = $8100 \pm 1100 L_{\odot}$. This value is somewhat unreliable, because the trajectory followed by the hydrogen reignition dogleg is itself a function of metallicity. If this effect is taken into account, the maximum luminosity may well be as low as $5500 L_{\odot}$.

In fact, both of these estimates will be too high if the population giving rise to the most luminous PN is old. Just how old can be estimated from the dynamical age of the OH-IR stars which, in a metal-rich environment like the Galactic Bulge, are

presumably the immediate precursors of PN. This has been done by te Lintel Hekkert (1990), who found that the dynamically young group of OH-IR stars have a mean dynamical age of 5 Gyr. In this case, from equations (5.1–5.3) L_{\max} (Galactic Bulge) = $5450 \pm 1000 L_{\odot}$. We adopt this value as our best estimate guess for L_{\max} . Clearly, any improvement in the theoretical estimate of L_{\max} would allow a corresponding improvement in the distance estimate, since the observational cutoff is far better determined than its theoretical value.

In Table 2, we give the distance estimate with these two extreme assumptions about the stellar age to show the sensitivity of our results on this paper. Our adopted distance to the Galactic Bulge is 7.6 ± 0.7 kpc; $(m - M)_0 = 14.4 \pm 0.2$. This is in good agreement with the value of 7.5 ± 0.9 kpc derived from globular clusters by Racine & Harris (1989), or the mean value of 7.7 ± 0.7 (Reid 1989), but clearly the older value of ~ 8.5 kpc (Harris 1976; Gunn et al. 1979; Quiroga 1981) is not excluded by our estimate.

6.3. PN in M31

The rich PN system in M31 and its companion dwarf elliptical galaxies has been very extensively studied by Ciardullo et al. (1989). The cutoff which they derived was converted to an apparent stellar luminosity F^* cutoff by correcting for mean extinction and for metallicity. For the reddening correction, we have taken $A(5007) = 3.56E(B - V)$ and have used an mean $E(B - V)$ of 0.11.

The correction for metallicity is somewhat more difficult, since although the [Fe/H] is quite well known, the [O/H] is not so well determined. We have taken [O/H] = 0.3. However, errors in this quantity will make little difference to the conversion efficiency of stellar flux to [O III] flux, since equation (4.1) and Figure 2 both indicate that the conversion efficiency is near its maximum. In this case, the conversion efficiency to 5007 Å luminosity is 13.7% and remains constant to within 15% for metallicities between twice solar and one-fourth solar. These estimates are slightly increased if the PNn did not evolve from C stars, which is likely in this higher metallicity regime. It is well known that in the Galaxy, for example, the ratio of the oxygen-rich and carbon-rich AGB stars is a strongly changing function of Galactocentric radius (Habing 1988; Jura & Kleinmann 1989, 1990). Within the solar circle, the large majority of AGB stars are of the oxygen-rich type. If the C/O ratio is taken to be solar (0.6) rather than 1.5, the maximum luminosity conversion factor is increased by a factor of 1.09 to 15.0%. We have adopted this value to derive the figure given in Table 2.

As for the Galactic Bulge, the age of the stars giving rise to the most luminous PN remains the most uncertain factor. In Table 2, we show the effect of assuming that star formation terminated 10 Gyr ago compared with the assumption that the youngest population has the same age as the OH-IR sources in our own Galaxy, 5 Gyr. This makes a 0.28 mag difference in distance modulus. Since we have no reason to prefer either of these estimates, we adopt the mean, with correspondingly greater error.

Once again, we find the PN distance scale to be somewhat smaller than the Cepheid distance (Welch et al. 1986; Freedman & Madore 1990); by ~ 0.18 mag in distance modulus. From the comparison of M31, LMC, and the SMC, it is clear that there is a systematic and metallicity independent zero-point shift of 0.14 mag, on average, between the two distance scales.

6.4. *The PN in the Virgo Ellipticals*

The PN in Virgo Ellipticals have been studied by Jacoby, Ciardullo, & Ford (1990). In Table 2, we have derived the mean apparent stellar luminosity cutoff F^* in exactly the same fashion as for M31.

Once again, effectively all the uncertainty in the distance derivation is in the calculation of the intrinsic luminosity, L_{\max} , of the stellar population which currently defines F^* . In Table 2, we investigate two extreme assumptions, first, that this population is like that of the Galactic Bulge, and second, that it is a 10 Gyr population with $[\text{Fe}/\text{H}] = +0.3$. This makes a difference of some 0.6 mag. Again, at the current time we have no reason to prefer one above the other of these assumptions, so we take the mean, giving the PN distance to the Virgo Cluster of 15.0 ± 2.0 Mpc, or $(m - M)_0 = 30.86 \pm 0.30$.

This result is in startlingly good agreement with that found by Jacoby, Walker, & Ciardullo (1990), $(m - M)_0 = 30.84$. However, this should not be so surprising, as this distance was found by comparing M31 and Virgo in a differential manner. Clearly, the stellar populations of these two systems are sufficiently similar for such a procedure to be valid. Our distance is also in good agreement with that given by the Tully-Fisher method, $(m - M)_0 = 30.85 \pm 0.40$, but is somewhat short compared with those derived by a number of other methods (see review by van den Bergh, 1989). We can shift our PN distance scale to a Cepheid distance scale by adding the +0.14 mag offset found above, to give $D_0 = 15.8 \pm 2.1$ Mpc, or $(m - M)_0 = 31.00 \pm 0.30$. This still gives a "short" distance scale, with a Hubble Constant (from Visvanathan 1990) of $84 \pm 11 \text{ km s}^{-1} \text{ Mpc}^{-1}$.

Based on this discussion, it is clear that, by making the appropriate corrections for metallicity and age, we have established relative distances of the LMC, the SMC, the galactic Bulge, M31, and the Virgo cluster by the use of the cutoff in the PN luminosity function. This calibration can be derived equally well from the $[\text{O III}]$ or Balmer line fluxes. Distances so derived are, within the errors, similar to those of the Cepheid

distance scale, where available. We conclude that the techniques for deriving extragalactic distances are well based upon stellar evolution and nebular plasma theory.

7. CONCLUSIONS

In this paper, we have shown that nebular modeling allows us to correct for metallicity and excitation effects to derive intrinsic apparent stellar luminosity functions of PNn using either observations in the $[\text{O III}]$ lines, or in the Balmer lines (or, equivalently, in the radio continuum). From these, it is clear that the upper luminosity cutoff is a good measure of the distance to the galaxy, provided that corrections for the age of the stellar population, and its metallicity can be accounted for.

This we have done, using theoretical evolutionary tracks which self-consistently deal with the evolution from the main sequence all the way through to the PN phase. Applying these to the observational H-R diagram of the LMC, and the luminosity functions of the LMC, SMC, Galactic Bulge, M31, and Virgo cluster populations, we have been successful in deriving distance moduli to each of these systems.

We find that the PN distance scale shows a systematic zero-point offset with respect to the Cepheid distance scale which appears to be independent of the metallicity or age of the parent stellar population.

The PN results favor a short distance scale on which the Virgo cluster lies within the range 13–18 kpc, and, correcting for the Cepheid zero-point offset, we find the Hubble Constant is to be $84 \pm 11 \text{ km s}^{-1} \text{ Mpc}^{-1}$.

Further refinement of the PN distance scale is dependent not so much upon the accuracy with which the upper luminosity cutoff can be established, but rather on a knowledge of the theoretical luminosity of the stars which are responsible for this cutoff. This in turn depends upon an accurate understanding of the age of this stellar population, and upon the core mass/initial mass relationship. These improvements are principally dependent upon the theory of stellar mass-loss and its dependence upon metallicity.

REFERENCES

- Binette, L., Dopita, M. A., & Tuohy, I. R. 1985, *ApJ*, 297, 476
 Brocato, E., Matteucci, F., Mazzitelli, I., & Tornambé, A. 1990, *ApJ*, 349, 458
 Caldwell, J. A. R., & Coulson, I. M. 1986, *MNRAS*, 218, 223
 Castellani, V., Chieffi, A., Pulone, L., & Tornambé, A. 1985, *ApJ*, 296, 204
 Caughlan, G. R., & Fowler, W. A. 1988, *Atomic Data & Nucl. Data*, 40, 283
 Cerruti-Sola, M., & Perinotto, N. 1985, *ApJ*, 291, 237
 Ciardullo, R., Jacoby, G. H., Ford, H. C., & Neill, J. D. 1989, *ApJ*, 339, 53
 Conti, P. S., Garmany, C. D., & Massey, P. 1986, *AJ*, 92, 48
 Dopita, M. A., Ford, H. C., Lawrence, C. J., & Webster, B. L. 1985, *ApJ*, 296, 390
 Dopita, M. A., & Meatheringham, S. J. 1990, *ApJ*, 357, 140
 ———. 1991a, *ApJ*, 367, 115
 ———. 1991b, *ApJ*, 377, 480
 Dopita, M. A., Vassiliadis, E., & Morgan, D. H. 1992, in preparation
 Evans, I. N., & Dopita, M. A. 1985, *ApJS*, 58, 125
 Feast, M. W. 1988 in *The Extragalactic Distance Scale*, ASP Conf. Ser. No. 4, eds. S. van den Bergh & C. J. Pritchett (Provo: Brigham Young Univ. Press), 9
 Feast, M. W., & Walker, A. R. 1987, *ARAA*, 25, 345
 Freedman, W. L., & Madore, B. M. 1990, *ApJ*, 365, 186
 Frogel, J. A., & Blanco, V. C. 1983, *ApJ*, 274, L57
 Gabler, R., Kudritski, R. P., & Mendez, R. 1991, in *Stellar Atmospheres: Beyond Classical Models*, ed. L. Crivellari, I. Hubeni, & D. G. Hummer (NATO ASI Ser.), 143.
 Gascoigne, S. C. B. 1969, *MNRAS*, 146, 1
 Gathier, R., Pottasch, S. R., Goss, W. M., & van Gorkam, J. H. 1983, *A&A*, 128, 325
 Gunn, J. E., Knapp, G. R., & Tremaine, S. D. 1979, *AJ*, 84, 1181
 Habing, H. J. 1988, *A&A*, 200, 40
 Harm, R., & Schwartzschild, M. 1975, *ApJ*, 200, 324
 Harris, W. E. 1976, *AJ*, 81, 1095
 Huebner, W. F., Mets, A. L., Magee, N. H., & Argo, M. F. 1977, *Astrophysical Opacity Library*, Los Alamos Scientific Obs. Rep., LA-6760-M
 Hutsemekers, D., & Surdej, J. 1989, *A&A*, 219, 237
 Hyland, A. R. 1991, *IAU Symp.* 148, *The Magellanic Clouds*, ed. R. Haynes & D. Milne (Dordrecht: Kluwer), 125
 Iben, I., Jr. 1984, *ApJ*, 277, 333
 Jacoby, G. H. 1980, *ApJS*, 42, 1
 ———. 1989, *ApJ*, 339, 39
 Jacoby, G. H., Ciardullo, R., & Ford, H. C. 1988, in *The Astrophysical Distance Scale*, ASP Conf. Ser., Vol. 4, ed. S. van den Bergh & C. J. Pritchett (Provo: Brigham Young Univ. Press), 42
 ———. 1990, *ApJ*, 356, 332
 Jacoby, G. H., Walker, A. R., & Ciardullo, R. 1990, *ApJ*, 365, 471
 Jura, M., & Kleinmann, S. G. 1989, *ApJ*, 341, 359
 ———. 1990, *ApJ*, 364, 663
 Laney, C. D., & Stobie, R. S. 1986, *MNRAS*, 222, 449
 Lattanzio, J. C. 1986, *ApJ*, 311, 708
 Meatheringham, S. J., Dopita, M. A., Ford, H. C., & Webster, B. L. 1988, *ApJ*, 327, 651
 Meatheringham, S. J., & Dopita, M. A. 1991a, *ApJS*, 75, 407
 ———. 1991b, *ApJS*, 76, 1085
 Meatheringham, S. J., Dopita, M. A., & Morgan, D. H. 1988, *ApJ*, 329, 166
 Monk, D. J., Barlow, M. J., & Clegg, R. E. S. 1988, *MNRAS*, 234, 583
 Paczyński, B. 1971, *Acta Astron.*, 21, No. 4, 417
 Pauldrach, A., Puls, J., Kudritski, R. P., Mendez, R. H., & Heap, S. R. 1988, *A&A*, 207, 123
 Pottasch, S. R. 1990, *A&A*, 236, 231
 Pottasch, S. R. 1984, *Planetary Nebulae: A Study of Late Stages of Stellar Evolution* (Dordrecht: Kluwer)
 Pottasch, S. R., & Acker, A. 1989, *A&A*, 221, 123
 Quiroga, R. J. 1980, *A&A*, 92, 186

- Racine, R., & Harris, W. E. 1989, *AJ*, 98, 1609
Reid, N. 1989, *Ap&SS*, 156, 73
Russell, S. C., & Bessell, M. S. 1989, *Ap&SS*, 70, 865
Russell, S. C., & Dopita, M. A. 1990, *ApJS*, 74, 93
———. 1992, *ApJS*, submitted
Sandage, A., & Tammann, G. A. 1990, *ApJ*, 365, 1
Sanduleak, N., MacConnell, D. J., & Philip, A. G. D. 1978, *PASP*, 90, 621 (SMP)
Schonberner, D. 1981, *A&A*, 103, 119
———. 1983, *ApJ*, 272, 708
Shaw, R. A. 1989 in *IAU Symp 131, Planetary Nebulae*, ed. S. Torres-Piembert (Dordrecht: Kluwer), 473
Stryker, L. L., & Butcher, H. R. 1981, in *IAU Colloq. 68, Astrophysical Parameters for Globular Clusters*, ed. A. G. Davis Philip & D. S. Hayes (Schenectady: L. Davis Press), 255
te Lintel Hekkert, P. 1990, Ph.D. thesis, University of Leiden
Tylenda, R., Stasinska, G., Acker, A., & Stenholm, B. 1991, *A&A*, 246, 221
van den Bergh, S. 1988, in *The Astrophysical Distance Scale*, ASP Conf. Ser., Vol. 4, ed. S. van den Bergh & C. J. Pritchett (Provo: Brigham Young Univ. Press), 375
Vassiliadis, E., & Wood, P. R. 2992, in preparation
Webster, B. L. 1988, *MNRAS*, 230, 377
Welch, D. L., McAlary, C. W., McLaren, R. A., & Madore, B. F. 1986, *ApJ*, 305, 583
Wood, P. R. 1991, in *Frontiers of Stellar Evolution*, ASP Conf. Ser., in press
Wood, P. R., & Faulkner, D. J. 1986, *ApJ*, 307, 659
Wood, P. R., Meatheringham, S. J., Dopita, M. A., & Morgan, D. H. 1987, *ApJ*, 320, 178
Wood, P. R., & Zarro, D. M. 1981, *ApJ*, 247, 247
Visvanathan, N. 1990, *Australian J. Phys.*, 43, 189
Zijlstra, A. A. 1989, Ph.D. thesis, University of Groningen